1993ApJ...409..110S

THE ASTROPHYSICAL JOURNAL, 409:110–125, 1993 May 20
© 1993. The American Astronomical Society. All rights reserved. Printed in U.S.A.

21 CENTIMETER STUDY OF SPIRAL GALAXIES IN CLUSTERS. III. NEUTRAL GAS CONTENT, STAR FORMATION, AND RADIO CONTINUUM PROPERTIES

MARCO SCODEGGIO[1]
Department of Astronomy, Cornell University, Ithaca, NY 14853-6801
AND
GIUSEPPE GAVAZZI
Osservatorio Astronomico di Brera, via Brera 28, 20121 Milano, Italy
Received 1992 August 17; accepted 1992 November 19

ABSTRACT

Twentyone centimeter line observations of 112 galaxies in seven clusters and in relatively isolated regions in the Coma "wall" were secured with the Arecibo[2] telescope. These, combined with an available data base, are used to discuss the relations between the neutral gas column density, the star formation rate, the FIR, and the radio continuum emission in spiral galaxies inside and outside rich clusters. It is found that hydrogen-deficient cluster galaxies have star formation rates similar to unperturbed isolated galaxies confirming that atomic gas ablation in clusters does not alter the supply of molecular gas. The extended radio continuum emission of about 30% of cluster spirals is higher than that of isolated galaxies of similar type at any given gas surface density. A significant fraction of these galaxies is found perturbed in its H I, optical, and radio continuum morphology consistent with the hypothesis that ram pressure, along with H I ablation, could produce major morphological disturbances as well as enhancements in the diffuse synchrotron emission due to magnetic field compression.

Subject headings: galaxies: evolution — galaxies: spiral — galaxies: stellar content — radio lines: galaxies — stars: formation

1. INTRODUCTION

Our understanding of the role played by the interstellar gas on the activity and evolution of spiral galaxies took great advantage from the multifrequency observational material that became available in the last decade. Observations of the H I line at 21 cm and of the various CO transitions in the millimeter bands provide us with measurements of the content and distribution of the interstellar gas in the primordial neutral and in the molecular forms (Haynes, Giovanelli, & Chincarini 1984; Young & Scoville 1991). Ultraviolet, optical, and near-infrared data trace the star formation activity and evolution (Kennicutt 1990). Radio continuum observations in the centimetric bands trace the cosmic rays accelerated by massive, newly born stars, thus giving indirect information on the star formation processes themselves (Gavazzi & Jaffe 1986). Far-infrared observations, finally, provide us with a measurement of the dust heating induced by the stellar population (Cox, Krugel, & Mezger 1986). Due to the complexity of the mutual interactions and feedback mechanisms in these processes, large observational samples are needed to constrain models of galaxy evolution. The optically selected sample of 883 CGCG spiral and irregular galaxies, included in the multifrequency data base presented in Gavazzi (1991), complemented with the new H I observations given in § 2 of this paper, represents a well-suited sample to approach this intricate question on sound statistical grounds and to study if and how the cluster environment has any relevant role in determining galaxy evolution. In fact, the data base contains galaxies in the nearby rich clusters A262, A1367, Coma, Virgo, A2147, and A2151 as well as a reference sample of noncluster objects (belonging to the Coma Supercluster "wall," outside the two main clusters, and to the Cancer region). The outline of the present paper is the following: in § 2 we present the newly obtained 21 cm observations taken at Arecibo. These data, combined with those already available in the 21 cm and in other bands are analyzed in § 3 with the aim of determining the relationships between the presence of neutral gas, the present star formation rate, and the FIR and radio continuum emissions in spiral galaxies in and outside rich clusters.

[1] Formerly at Osservatorio Astronomico di Brera, Milano, Italy.

[2] The Arecibo Observatory is part of the National Astronomy and Ionosphere Center, which is operated by Cornell University under cooperative agreement with the National Science Foundation.

2. OBSERVATIONS AND DATA REDUCTION

Twentyone centimeter observations of 112 galaxies were obtained with the Arecibo 305 m telescope in 32 periods of about 3 hr duration from 1991 January 1 to 31. A dual-channel HEMT receiver was used in conjunction with the 22 cm tunable feed to observe galaxies with $cz > 1500$ km s^{-1} and with cz unknown (search mode). Seven galaxies with $cz < 1500$ km s^{-1} were observed using the 21 cm circular feed tuned at 1407 MHz, coupled with a dual-channel HEMT receiver. Data taking and reduction have been described in Paper I and II of this series (Gavazzi 1987, 1989). Observations were obtained in the beam-switching mode by observing the object (ON scan) during half of the integration time and the blank sky in the other half (OFF scan) at equal azimuth and zenith angle. ON-OFF pairs, each of 10 minute duration, were repeated and accumulated until a signal-to-noise ratio high enough (typically ≥ 10) to allow accurate determinations of the line width was obtained. The observations were made with the 2048 channel autocorrelation spectrometer split into four subcorrelators of 512 channel, each with 20 MHz bandwidth. Each polarization fed two subcorrelators. In search mode (i.e., for

© American Astronomical Society • Provided by the NASA Astrophysics Data System

1993ApJ...409..110S

TABLE 1

PARAMETERS OF THE DETECTED GALAXIES

Name (1)	UGC (2)	NGC (3)	R.A. (4)	Dec. (5)	T (6)	mp (7)	a (8)	b (9)	Vo (10)	Vr (11)	W20 (12)	W50 (13)	rms (14)	SHI (15)	q (16)	Cluster (17)
-	30	-	000158.40	331650.0	9	16.0	1.2	0.2	4760	4762	272	260	1.19	2.54	1	-
499072	108	-	000909.60	281318.0	5	14.8	1.0	0.5	-	8044	413	409	0.63	0.91	1	-
500008	215	-	001949.00	291333.0	3	14.9	1.3	0.8	7091	7062	423	419	0.68	2.00	1	-
500001	285	-	002613.50	283953.0	3	15.0	1.0	0.3	-	2184	151	149	0.58	0.47	1	-
522023	-	-	014823.67	343729.3	9	15.5	0.7	0.3	4499	4685	247	240	1.77	3.09	1	A262
522023S	1316	-	014824.00	343600.0	9	16.5	0.6	0.2	-	4685	247	240	1.77	3.09	1	A262
522065	-	-	015217.77	351245.9	3	15.6	0.8	0.3	-	5709	445	436	0.70	1.38	1	A262
522081	1416	-	015348.33	363835.7	5	14.9	1.3	0.7	5314	5473	410	397	1.14	2.30	1	A262
522096	1459	-	015609.18	354914.4	7	15.4	1.6	0.2	-	5468	394	393	1.14	1.51	1	A262
-	2507	-	030040.00	302530.0	7	16.5	1.1	0.4	16091	16087	513	500	0.70	2.85	1	-
506006	2525	-	030235.10	331200.0	9	15.6	1.0	0.3	6228	6224	404	403	1.44	8.20	1	-
-	2868	-	034521.00	345930.0	6	17.0	1.8	0.2	-	5423	427	424	1.26	1.44	1	-
-	2882	-	034925.00	343212.0	8	17.0	1.8	0.7	-	4276	220	210	1.53	4.81	1	-
-	2915	-	035646.00	322830.0	7	17.0	1.2	0.2	5302	5307	342	319	1.89	5.98	1	-
119019	-	-	081225.60	214244.0	9	15.7	1.0	0.2	4276	4272	297	290	0.54	1.31	1	Cancer
119028	-	-	081430.20	211909.0	8	15.5	0.8	0.4	2156	2156	184	172	1.16	4.61	1	Cancer
119035	-	-	081500.20	223532.0	9	15.4	0.9	0.3	2122	2096	167	150	0.64	1.47	1	Cancer
119040	-	-	081531.00	205639.0	2	15.6	0.5	0.3	4811	4816	315	312	0.38	0.83	1	Cancer
119041	4324	-	081534.70	205505.0	9	15.3	1.6	0.6	4787	4817	-	-	0.42	1.44	1	Cancer
119051	-	-	081618.30	205452.0	5	15.5	0.8	0.4	5031	5028	247	226	0.60	1.72	1	Cancer
119057	4334	2565	081652.20	221122.0	5	13.8	1.8	0.7	3585	3584	430	426	1.32	12.53	1	Cancer
119059	-	-	001703.90	211328.0	9	15.7	0.6	0.2	4248	4221	237	224	0.42	0.84	1	Cancer
119068	4354	2570	081827.20	210414.0	3	15.4	1.3	0.7	6541	6562	318	312	0.81	2.97	1	Cancer
119078	4375	-	082014.82	224935.9	7	14.6	2.7	1.8	2059	2061	301	297	1.53	9.66	1	Cancer
119080	4383	2339	082037.50	212958.0	8	15.2	0.5	0.3	5348	5423	316	291	0.86	5.28	1	Cancer
-	5392	-	095848.00	215100.0	7	16.0	1.2	0.2	-	6209	404	385	0.60	1.49	1	-
-	5401	-	095946.00	191618.0	8	17.0	1.4	0.6	-	2002	150	148	1.28	4.69	1	-
93001	5426	-	100146.70	150030.0	7	15.4	1.5	0.1	-	6976	440	438	0.63	2.41	1	-
-	5431	-	100212.00	214648.0	7	16.0	1.3	0.2	-	3965	212	206	1.07	3.99	1	-
93002	5471	-	100552.00	182833.0	5	14.0	2.3	0.7	5251	5102	551	546	1.05	4.89	1	-
93003	5495	-	100910.00	164130.0	7	14.7	3.0	0.3	-	8248	574	571	1.00	11.32	1	-
93004	5514	-	101100.00	182200.0	7	15.5	1.2	0.2	-	3655	203	196	1.19	3.82	1	-
93005	5552	-	101442.00	172030.0	6	15.0	1.6	0.3	-	8293	488	482	0.65	1.97	1	-
97008	-	-	113034.23	200401.1	9	15.7	0.8	0.2	-	9780	439	431	0.99	2.38	1	-
157003	-	-	113453.19	313821.1	8	14.6	0.8	0.7	12730	12727	278	246	0.64	3.51	1	-
97052	6636	3802	113743.02	180234.9	9	14.7	1.2	0.3	3200	3240	278	259	0.95	1.06	3	-
127034	-	-	114019.87	232421.7	9	15.5	0.8	0.5	8696	8684	306	287	0.57	1.93	1	Comasup
127035	6681	-	114025.79	241319.0	9	15.4	1.2	0.3	-	6817	466	457	0.57	1.57	1	Comasup
157026	-	-	114123.87	301908.4	3	15.4	0.9	0.4	11767	11787	534	521	0.75	2.53	1	-
97151	-	-	114452.98	181955.3	9	15.6	0.7	0.2	-	5854	401	394	0.46	0.78	1	Comasup
157033	-	-	114520.80	282047.0	9	15.6	0.8	0.3	-	8882	306	284	1.14	2.57	1	Comasup
97174	-	-	115009.33	185335.2	9	15.7	0.7	0.3	-	7877	260	257	0.94	2.18	1	Comasup
98001	-	-	115139.23	201816.5	9	15.6	0.7	0.3	-	6206	243	240	0.64	1.60	1	Comasup
98007	-	-	115310.57	180957.3	9	15.5	0.9	0.4	6346	6350	327	322	1.12	4.29	1	Comasup
127111	-	3997	115452.50	253040.1	6	15.7	0.6	0.3	4713	4629	518	511	0.80	3.39	4	-
157080	-	-	115742.37	313009.4	8	14.8	0.8	0.4	714	617	132	117	1.24	2.64	2	-
157085	-	-	115829.87	310721.1	9	15.7	0.7	0.4	-	3117	135	126	1.19	1.65	1	-
98051	7074	-	120249.99	181152.7	9	14.6	1.0	0.3	4248	4283	432	420	1.08	4.15	4	-
98069	7133	-	120646.73	191630.9	7	15.5	1.6	1.0	2167	2578	210	195	1.28	4.77	1	-
98093	-	-	120925.06	201821.6	9	15.3	0.7	0.4	-	2400	201	183	2.10	5.17	1	-
158042	-	-	120952.40	290542.0	9	14.8	0.9	0.5	4050	3868	254	226	0.91	1.28	2	-
158096	7459	-	122043.80	291013.0	7	15.6	2.4	0.2	587	567	182	174	1.15	2.94	1	-
158101	7505	-	122248.00	265931.0	8	15.4	1.5	0.3	331	314	140	138	1.38	13.30	2	-
159004	-	3406	122633.19	275500.7	9	15.7	0.7	0.4	-	7004	276	275	0.75	0.63	2	Comasup
159018	7750	-	123241.25	300108.0	6	15.1	1.4	0.5	8055	8061	452	451	0.99	3.90	1	Comasup
129008	7758	4562	123306.91	260742.5	7	14.6	2.4	0.8	1379	1351	150	138	1.03	6.57	1	-
159054	-	-	123846.30	270037.0	9	15.5	0.7	0.4	4477	4759	230	216	0.96	2.49	1	-
159067	-	-	124211.50	284444.0	9	14.7	0.9	0.5	993	943	91	91	1.16	6.89	2	-
160001	-	-	125126.20	291459.0	9	15.6	0.7	0.3	7890	7945	330	311	0.55	1.26	1	Coma
130004	-	-	130123.64	262127.6	9	15.7	0.8	0.4	11206	11260	364	348	0.72	1.99	1	-
160126	-	-	130203.70	265623.0	9	15.3	0.7	0.3	10820	10794	451	445	0.72	2.14	1	-
160139	-	-	130414.62	290700.8	8	15.0	1.0	0.6	4761	4748	221	201	1.12	4.28	2	Coma

© American Astronomical Society • Provided by the NASA Astrophysics Data System

1993ApJ...409..110S

TABLE 1—*Continued*

Name (1)	UGC (2)	NGC (3)	R.A. (4)	Dec. (5)	T (6)	mp (7)	a (8)	b (9)	Vo (10)	Vr (11)	W20 (12)	W50 (13)	rms (14)	SHI (15)	q (16)	Cluster (17)
160153	-	-	130737.30	301822.0	8	15.4	0.9	0.3	10459	10457	415	407	0.84	1.63	3	-
101006	8248	-	130800.25	184214.9	5	14.8	1.1	0.4	3860	3705	296	286	1.11	10.38	1	-
130024	8336	4215	131353.25	254008.2	4	15.0	1.6	0.3	3790	3891	389	378	0.72	0.52	3	-
161041	-	-	132122.30	315421.0	9	15.5	0.8	0.4	5016	4979	179	172	0.55	0.61	1	-
161045	-	4239	132205.94	311309.5	9	15.3	0.8	0.5	14578	14522	555	553	0.65	2.38	1	-
101045	-	-	132352.01	180059.7	9	15.5	0.7	0.4	8529	8332	287	257	0.58	1.88	2	Comasup
161052	-	-	132430.00	265101.5	9	15.1	0.3	0.3	7073	7072	345	339	0.67	1.38	2	Comasup
131008	8457	-	132506.29	210820.0	6	15.6	1.2	0.2	5966	5972	437	430	1.00	3.89	1	Comasup
161063	8466	-	132607.00	310427.0	8	15.5	1.3	0.6	7137	7300	311	301	1.10	4.40	1	Comasup
101061	8507	-	132834.12	194143.4	8	14.0	1.6	0.9	1020	999	116	107	1.14	4.99	2	-
108016	10101	6018	155512.49	160057.9	3	14.6	1.4	0.7	5121	5147	179	138	0.87	0.59	3	-
108027	-	-	155611.34	181053.2	9	15.7	0.9	0.3	-	12642	474	464	0.75	0.54	4	A2151
108031	-	-	155635.70	150725.9	9	15.6	0.9	0.4	10527	10602	442	438	0.68	2.99	2	A2147
108097	10169	-	160213.38	145716.2	8	15.2	2.5	0.4	4579	4642	170	161	0.61	0.37	3	-
108132W	10193	-	160327.96	162013.9	9	15.7	1.0	0.2	12512	13052	708	682	0.44	2.02	1	A2147
108132E	-	-	160329.78	161949.8	9	16.0	0.4	0.2	-	12061	241	220	0.44	0.68	1	A2147
108139	-	-	160345.83	181948.3	6	15.7	1.0	0.5	11215	11209	586	585	0.59	1.22	1	A2151
108146	-	-	160400.60	183253.0	7	15.7	0.8	0.6	11161	11133	399	391	0.38	0.69	1	A2151
108156	10215	-	160512.90	194053.0	9	15.7	1.0	0.7	7805	7798	269	260	1.06	2.62	1	-
108157	-	-	160554.79	165412.5	9	15.7	0.9	0.4	-	11552	526	516	0.42	1.10	1	A2147
140001	10837	-	172240.30	250030.0	5	15.0	2.0	0.9	-	8182	426	420	1.16	7.18	1	-
111018	10873	-	172700.90	161207.0	8	15.2	1.5	0.2	-	5992	352	350	1.20	2.99	1	-

NOTES.—The Coma Supercluster (Comasup) is defined as the region limited by $11^h30^m \leq \alpha \leq 13^h30^m$; $18° \leq \delta \leq 32°$ and $5300 \leq cz \leq 9000$ km s^{-1}.

Comments on individual objects: UGC 30, UGC 215, UGC 2507, UGC 2525, and UGC 2915 were observed by Giovanelli & Haynes 1989. The observations were repeated to determine the shape of their profiles (unpublished). The two sets of data are in full agreement.

522023: the galaxy lies 1.'5 north of 522023S (UGC 1316). The two galaxies are within the Arecibo beam. Both galaxies have spiral morphology, but 522023 has a brighter bulge (possibly S0a). The H I emission cannot be attributed unambiguously to one object.

522065, 522096: data include some pairs kindly provided by R. Giovanelli (private communication).

119059, 119061, 119040, 119082: undetected by Bothun et al. 1985. Due to the better signal-to-noise ratio of our observations two of them (119040, 119059) were detected and two remained undetected with more stringent upper limits.

119040 and 119041 are in the same beam. Unfortunately, due to similarity of the redshifts, the H I emission is overlapped (see three-horn profile in Fig. 1).

119080W: in contact with 119080E. The redshifts are 5348 and 5219 km s^{-1}, respectively. CCD observations reveal that both galaxies have a spiral structure, but, due to its larger size, we are inclined to attribute the H I flux to 119080E.

97008 lies at about 1.'5 from 97009; therefore, a possible contribution from 97009 cannot be excluded. Moreover, the redshift of 97009 is unknown. However, repeated observations using offset pointing indicate that the reported H I flux is associated with 97008.

127111: member of the NGC 4005 group. Our profile is in close agreement with the one obtained by Williams 1986. The measurement is confused by the emission from 127110 and 127112, which lie about one beam away from 127111 and have velocities similar with the one under study. 127110 was observed by Gavazzi 1987 and Williams 1986 with $V = 4495$ and $W = 575$. 127112 lies at $V = 4828$ and $W = 364$.

98051: confused with 98050. Gavazzi 1987 observed both galaxies and found that the two peaks at higher velocity in Fig. 1 belong to 98050. 98051 has a lower systemic velocity, but its width is undetermined.

108132W and 108132E were detected in the same beam. However, the two galaxies are well resolved in frequency (see Fig. 1).

We wish to point out two errors we detected in Paper I of this series (Gavazzi 1987). Galaxy 97064 should be considered undetected. The H I flux attributed to this galaxy was in fact due to 97068 lying at 2.'2 from it. The velocity of 157035, $V = 6371$, was mistyped. The corrected value is $V = 6281$.

galaxies of unknown redshift), the two subcorrelators on each polarization were offset by 15 MHz, thus allowing a 5 MHz overlap. This resulted in a total search bandwidth of 35 MHz, generally centered at 5500 km s^{-1}, thus covering a search interval 1500–8500 km s^{-1}. To avoid severe interference at 1330 and 1350 MHz caused by the FAA radar serving the San Juan airport a radar blanker was used. This instrument flags the data taking when the radar transmitter is on, with the drawback that the integration time increases by about 20%.

The observed galaxies were mainly selected from the CGCG (Zwicky et al. 1961–1968) inside the contours of the clusters A262, A1367, Coma, and Hercules (A2147 and A2151) and in the relatively isolated regions of Cancer and of the Coma Supercluster. Some other galaxies lying within 15° projected radii from A262, Cancer, and Hercules were selected from the UGC catalog (Nilson 1973). Galaxies with large inclination were preferred for the purpose of obtaining measurements useful also for studies based on the Tully-Fisher relation (Tully & Fisher 1977), partly included in Gavazzi et al. (1991b, 1992). Observations of some objects already available in the literature were repeated to improve their quality or if their profiles were unpublished.

Eighty-three objects were detected, including 28 for which new redshifts were obtained. These are listed in Table 1 as follows (see Paper I and II for more details).

Cols. (1)–(3): CGCG (Zwicky et al. 1961–1968), UGC (Nilson 1973), and NGC (de Vaucouleurs et al. 1991 [RC3]) names.

Cols. (4)–(5): 1950 optical celestial coordinates. These were in most cases measured with a second of arc accuracy using the Bologna X-Y measuring engine, or taken from Basso et al. (1990) and from Santagata et al. (1987).

© American Astronomical Society • Provided by the NASA Astrophysics Data System

1993ApJ...409..110S

Col. (6): Morphological type (3 = Sa, 4 = Sab, 5 = Sb, 6 = Sbc, 7 = Sc, 8 = Irr, 9 = S ...) from the literature or estimated by eye inspection on the available plate material.

Col. (7): Photographic magnitude from the CGCG or from the UGC.

Cols. (8)–(9): blue major and minor axes (in minutes of arc). These were taken from the UGC or measured consistently on the blue copy of the Palomar Sky Survey plates.

Col. (10): heliocentric velocity previously available.

Columns (11)–(16) report the newly obtained 21 cm data.

Col. (11): heliocentric systemic velocity derived by averaging the velocity determined at 20% of the peak with the value at 50% of the mean of the profile.

Col. (12): observed width (km s^{-1}) of the profile, measured at 20% of the peak flux.

Col. (13): observed width (km s^{-1}) of the profile, measured at 50% of the mean flux.

Col. (14): rms noise in the smoothed profile (in mJy).

Col. (15): measured H I line integral intensity in Jy km s^{-1}. The fluxes of galaxies with major diameter greater than 1.'8 should be corrected for partial resolution by the 3.'3 Arecibo beam according to Sullivan et al. (1981). No corrections for internal absorption and pointing errors have been included. The latter is estimated in 5%.

Col. (16): quality of the obtained profile. Quality 1 are high signal-to-noise two-horned profiles. Quality 2 are high signal-to-noise single-horned profiles. Quality 3 are marginal profiles and Q = 4 are poor spectra. Q = 1, 2 profiles are useful for deriving distances using the Tully-Fisher relation.

Col. (17): cluster membership.

Figure 1 shows the smoothed (20 km s^{-1} resolution) spectra of the detected galaxies.

Table 2, arranged similarly to Table 1, lists the 29 undetected galaxies. Twenty have redshift for which a useful upper limit to the H I mass can be obtained. The remaining nine undetected galaxies were searched in the interval 1500–8500 km s^{-1}, with typical rms of 1 mJy. These are not used in the following discussion. Among the undetected objects there are still many galaxies in the A262 Cluster due to their declination near the limit of the Arecibo telescope. Much improved observations of this cluster will be possible after the completion of the Gregorian upgrade of the telescope.

3. RESULTS AND DISCUSSION

This section is devoted to the analysis of the relationships between the galaxy H I content and the star formation rate derived from the Hα emission line, and between the H I content and the centimetric radio continuum and far-infrared (FIR) emissions. In order to avoid trivial conclusions such as "bigger galaxies have more of everything," which are simply a consequence of a scaling law, and to derive distance-independent parameters, all measured quantities are normalized to some indicator of the overall galaxy size or luminosity. The radio continuum and FIR fluxes are normalized to the near-infrared *H*-band flux, giving the ratios radio/*H* and FIR/*H*. Similarly the 21 cm line flux is normalized to the optical galaxy area, yielding to a hybrid surface density. The flux measured in correspondence of the Hα + [N II] lines is normalized to the continuum near 6570 Å, yielding to the Hα equivalent width (EW).

TABLE 2

PARAMETERS OF THE UNDETECTED GALAXIES

Name (1)	UGC (2)	NGC (3)	R.A. (4)	Dec. (5)	T (6)	mp (7)	a (8)	b (9)	Vo (10)	Vr (11)	W20 (12)	W50 (13)	rms (14)	SHI (15)	q (16)	Cluster (17)
522012	-	-	014625.34	355927.2	2	15.7	0.9	0.3	4041	-	-	-	2.36	-	-	A262
522053	-	-	015059.89	362342.3	9	15.4	0.7	0.3	4556	-	-	-	2.56	-	-	A262
522054	-	-	015114.78	354038.1	3	15.2	0.6	0.3	4522	-	-	-	1.11	-	-	A262
522066	1390	-	015224.29	350342.3	6	15.5	1.0	0.2	4380	-	-	-	1.51	-	-	A262
522080	1415	-	015346.55	360826.2	9	14.5	1.1	0.3	4796	-	-	-	0.89	-	-	A262
522084	1434	-	015441.49	360041.3	5	15.4	1.5	0.5	4589	-	-	-	1.20	-	-	A262
522097	1460	-	015607.32	360058.0	3	15.0	1.5	0.9	4937	-	-	-	1.43	-	-	A262
119061	-	-	081715.80	211337.0	5	15.5	0.6	0.5	5191	-	-	-	0.48	-	-	Cancer
119082	-	-	082100.60	210815.0	3	15.6	0.8	0.4	4715	-	-	-	0.68	-	-	Cancer
119101	-	-	082406.00	215218.9	9	14.8	0.7	0.3	4597	-	-	-	0.60	-	-	Cancer
127008	6598	3772	113511.87	225806.2	3	14.4	1.2	0.6	3478	-	-	-	0.81	-	-	-
97069	-	-	113956.11	180342.7	8	15.6	0.6	0.2	-	-	-	-	1.20	-	-	?
127059	-	-	114614.64	220206.0	9	15.6	0.9	0.5	9809	-	-	-	0.97	-	-	-
97168	-	-	114913.57	193812.3	9	15.7	0.7	0.2	-	-	-	-	1.20	-	-	?
127085	-	-	114955.74	205412.9	9	15.5	0.9	0.4	6595	-	-	-	1.05	-	-	Comasup
128040	-	-	120622.50	252811.6	9	15.1	0.7	0.4	6852	-	-	-	0.62	-	-	Comasup
98074	-	-	120725.28	201146.0	9	15.6	0.7	0.4	-	-	-	-	1.20	-	-	?
128066	-	3075	121323.12	235223.9	9	15.1	0.9	0.5	-	-	-	-	1.38	-	-	?
159104	-	-	125050.00	272157.0	9	15.0	0.8	0.5	6154	-	-	-	0.84	-	-	Coma
160007	-	4788	125150.20	273427.0	9	15.4	0.9	0.4	6462	-	-	-	0.67	-	-	Coma
160018	-	-	125302.30	275535.0	9	15.3	0.8	0.3	7092	-	-	-	0.67	-	-	Coma
160114	-	-	130016.70	283821.0	9	15.6	1.0	0.3	7454	-	-	-	0.56	-	-	Coma
160142	-	-	130503.60	265925.0	8	15.5	0.7	0.4	11301	-	-	-	0.89	-	-	-
160191	-	-	131639.62	310444.6	9	15.7	0.7	0.3	-	-	-	-	1.30	-	-	?
101043	8437	-	132254.62	184243.3	3	15.0	1.0	0.3	6677	-	-	-	0.66	-	-	-
108057	-	-	155901.48	175423.8	3	15.6	0.6	0.4	10378	-	-	-	0.57	-	-	A2151
108074	-	-	160004.72	161748.1	9	15.6	0.9	0.3	12894	-	-	-	0.70	-	-	A2147
108143	-	-	160402.92	164017.4	9	15.7	0.6	0.3	10785	-	-	-	0.43	-	-	A2147

NOTES.—See notes to Table 1.

© American Astronomical Society • Provided by the NASA Astrophysics Data System

1993ApJ...409..110S

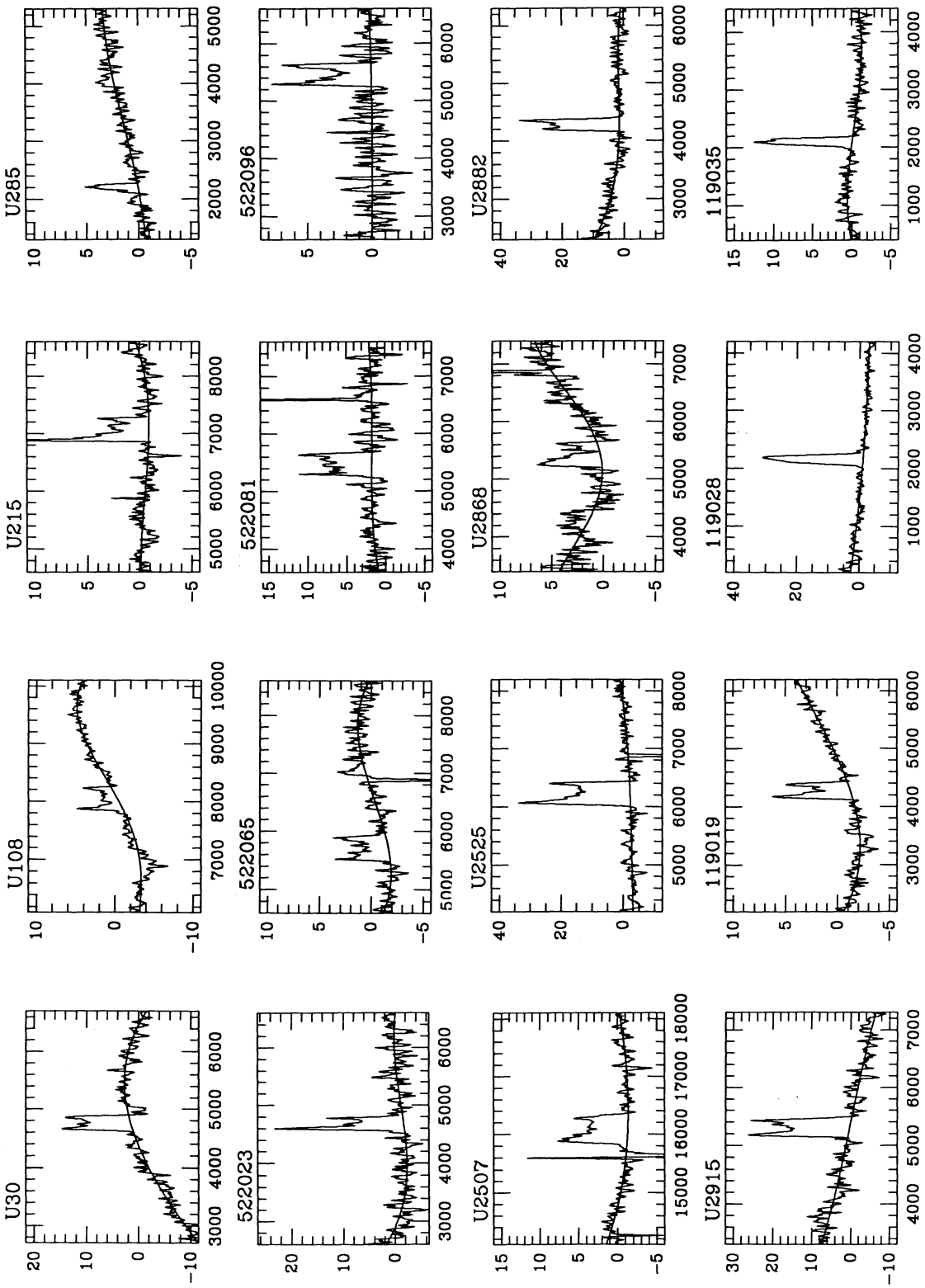

FIG. 1.—Smoothed H I profiles of the 83 detected galaxies. Fitted baselines are superposed. The frequency axes is labeled in km s^{-1}; the flux is in mJy.

© American Astronomical Society • Provided by the NASA Astrophysics Data System

1993ApJ...409..110S

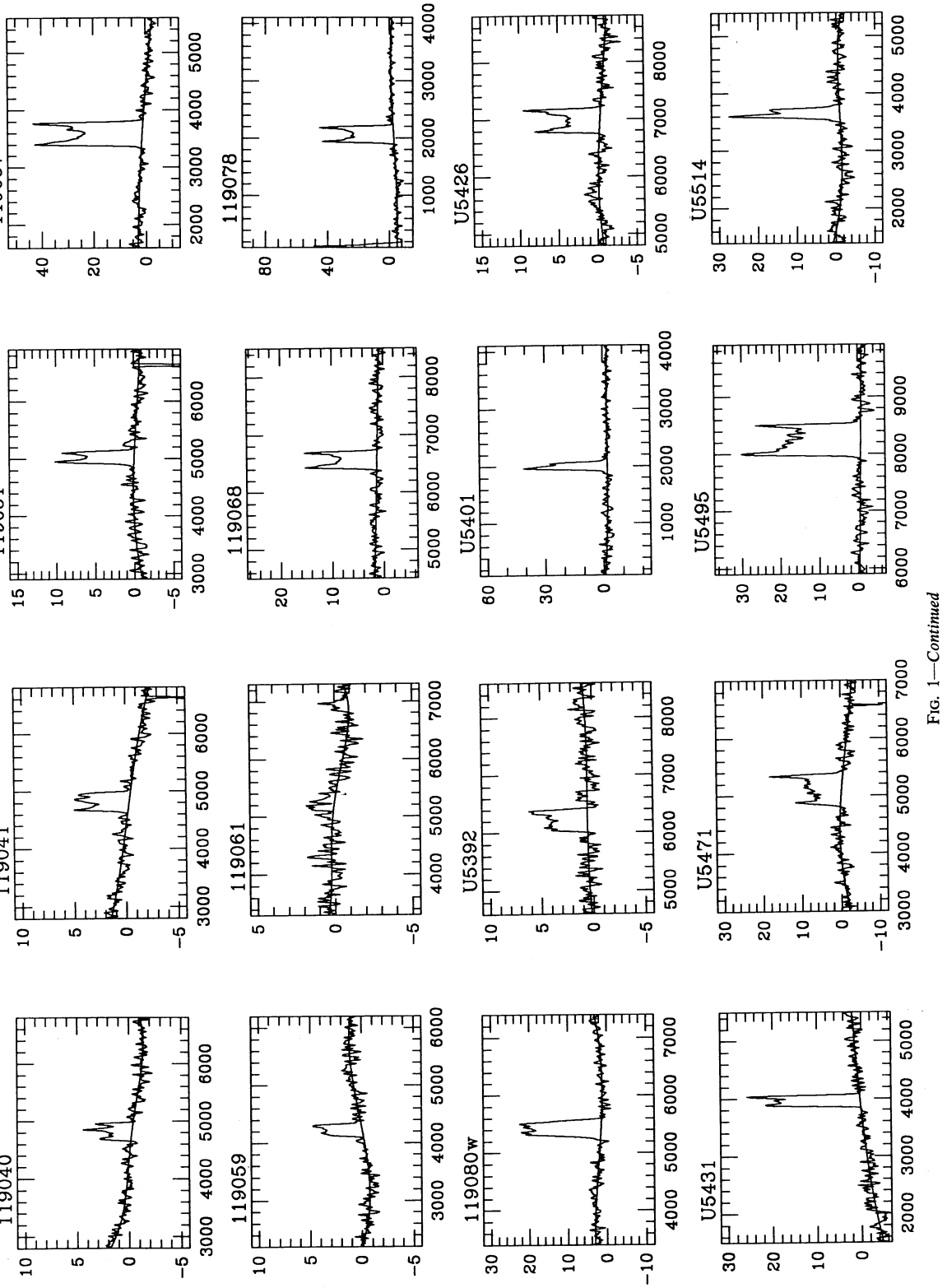

FIG. 1—*Continued*

© American Astronomical Society • Provided by the NASA Astrophysics Data System

1993ApJ...409..110S

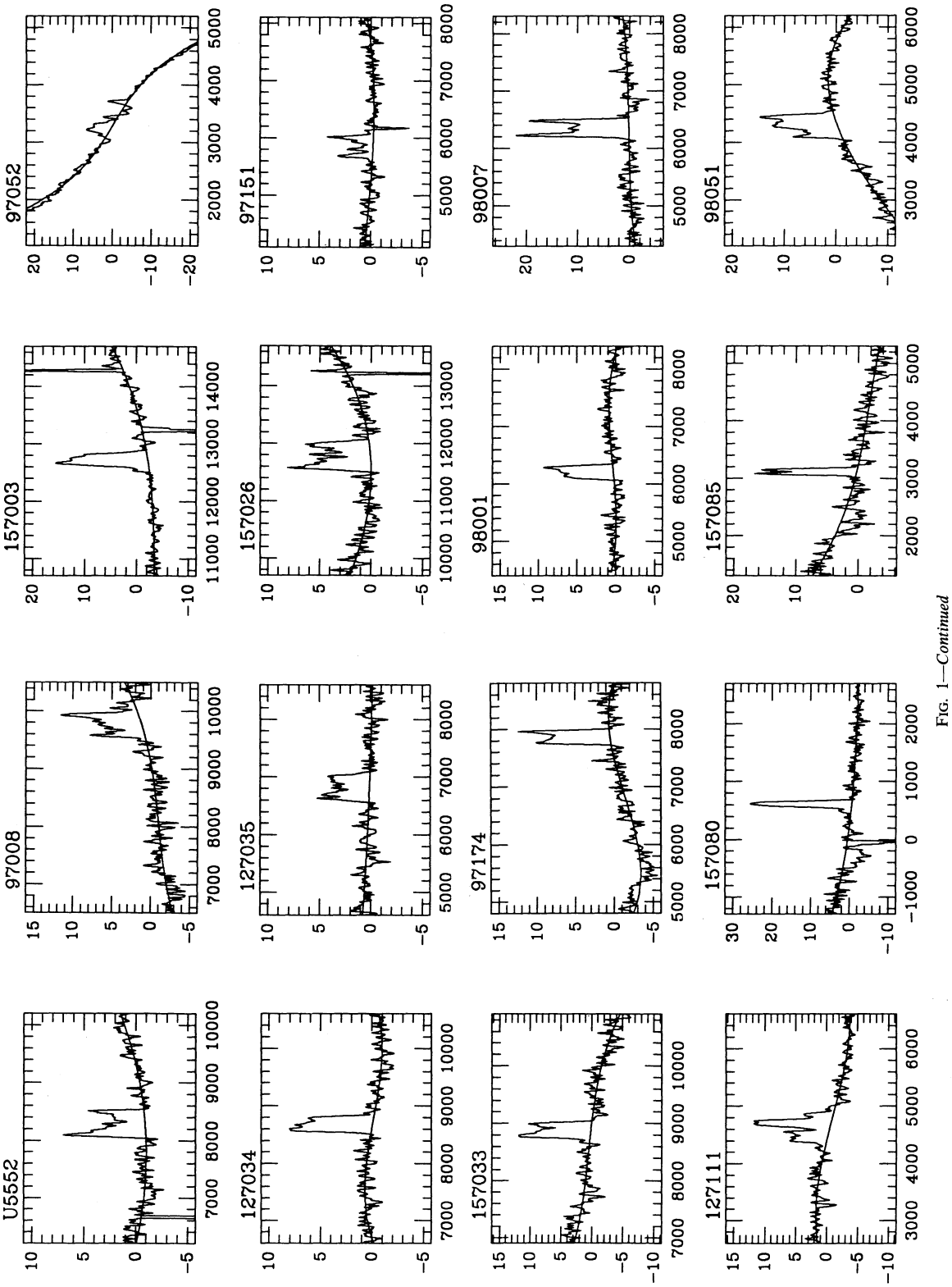

FIG. 1—*Continued*

© American Astronomical Society • Provided by the NASA Astrophysics Data System

1993ApJ...409..110S

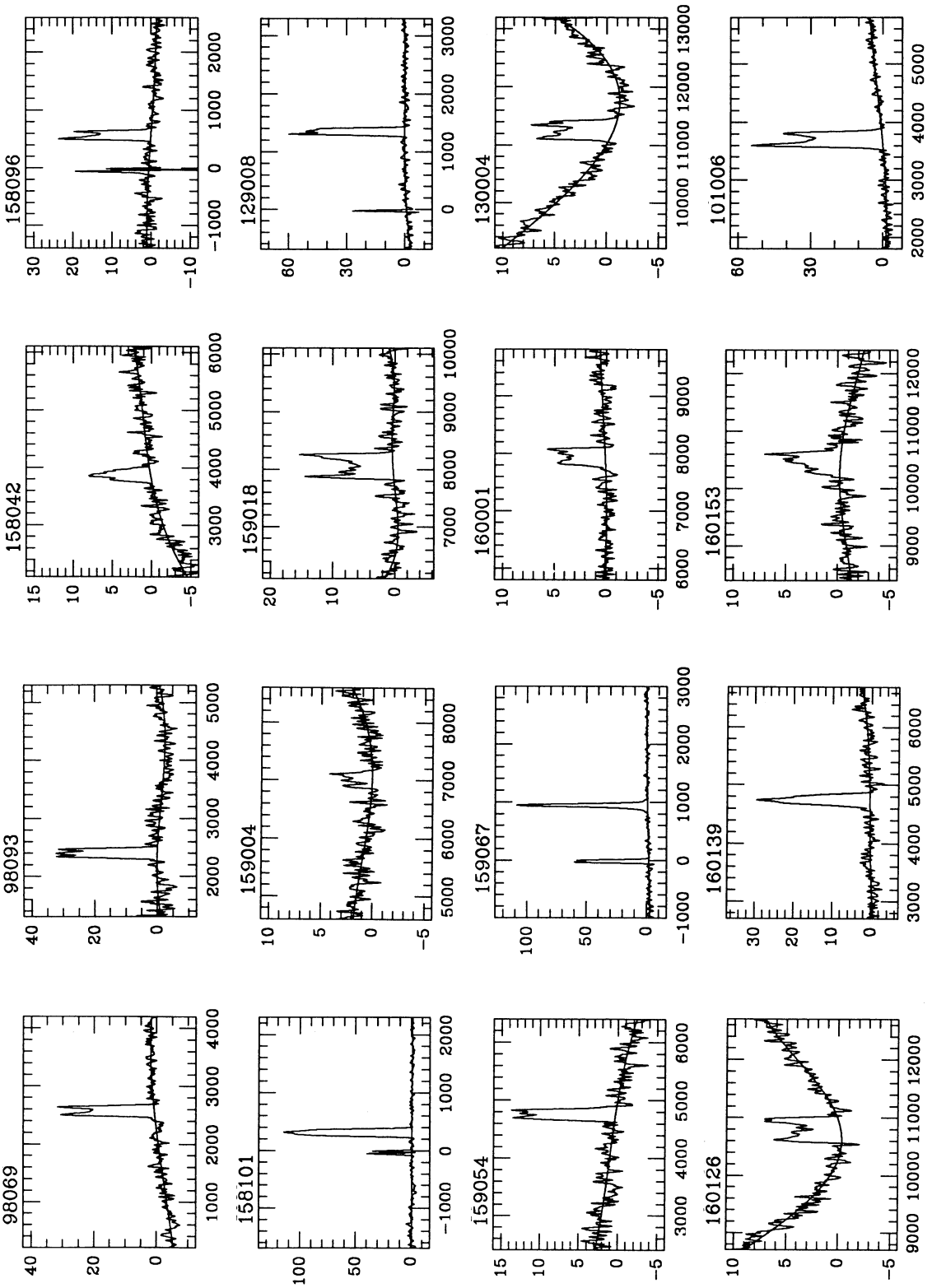

FIG. 1—*Continued*

© American Astronomical Society • Provided by the NASA Astrophysics Data System

1993ApJ...409..110S

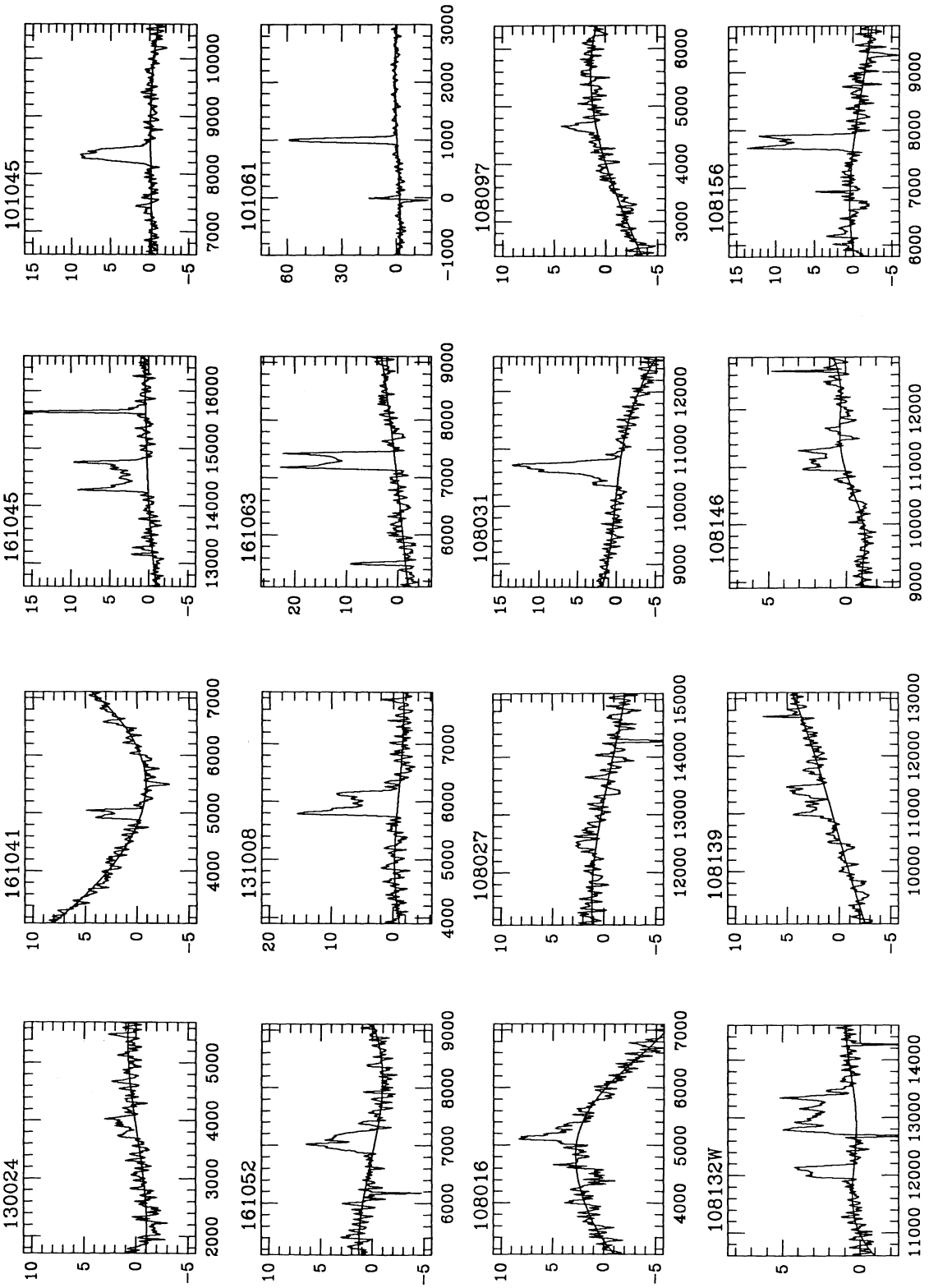

FIG. 1—*Continued*

© American Astronomical Society • Provided by the NASA Astrophysics Data System

1993ApJ...409..110S

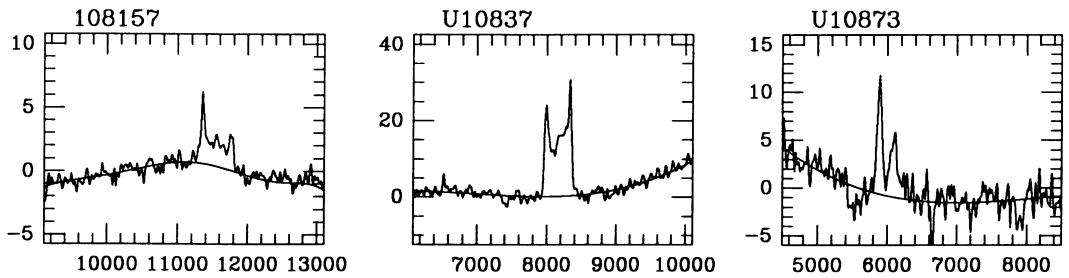

FIG. 1—*Continued*

The data base of 883 spiral galaxies available to us, although is far from complete, contains a conspicuous number of objects with reliable photometrical measurements which are suitable for statistical studies. Table 3 reports the available radio continuum (carried out mainly at 1415 MHz, and some, obtained at 610 MHz, converted to 1415 assuming a spectral index of −0.8), H I line and FIR (60 μm) measurements. The latter have been taken from the literature except in the Coma Supercluster region where they have been derived by us using the *IRAS* faint source data base. The table reports in columns (1) and (2) the number of surveyed objects separately from those actually detected, the difference being constituted by upper limits. Five-hundredfortyone of the 883 spirals have *H*-band magnitudes available, allowing us to derive normalized quantities, as reported in columns (3) and (4) of Table 3. Observation of the Hα line are unfortunately very incomplete, as only 165 objects have reliable measurements of the Hα EW. Detailed references to the above measurements are not given for conciseness. However they are included in the data base which is available in a computer readable form upon request from the authors.

3.1. H I *Surface Density and Star Formation Rate*

The EW of the Hα line is the most widely used tracer of the star formation rate (SFR) in galaxies, despite the fact that it traces stars only above 10–15 $M_\odot$, i.e., only a fraction of nearly 10%–20% of the total stellar mass, if a conventional IMF is assumed (see a review in Kennicutt 1990). This, in conjunction with the somewhat uncertain amount of extinction that occurs within galaxies themselves, contributes to an uncertainty of the order of 50% in the determination of the SFR in individual galaxies, even though the flux measurements and EW determinations have typical intrinsic accuracies of 10% (Kennicutt 1983a).

The simple model proposed by Schmidt (1959), which relates the SFR to the local gas density Σ, according to a power law

$$\mathrm{SFR} = a\Sigma^{\alpha}$$

has been questioned by several authors who proposed a non-linear dependence of these two quantities (Guiderdoni 1987; Kennicutt 1989). In particular, Kennicutt (1989), analyzing the H I, CO, and Hα emission from nearby spatially resolved galaxies, showed that a direct proportionality between SFR and gas surface density exists only at high gas densities, whereas the relation is strongly nonlinear at low and intermediate densities: i.e., there is a threshold in the gas density below which the star formation activity does not take place (cf. Fig. [8] in Kennicutt 1989). Our sample is dominated by distant objects; therefore our analysis does not include many spatially resolved observations. Instead it is based on integrated measurements, both for Hα EW and gas content. Moreover, only a small number of these galaxies have been observed in CO to make possible a direct determination of their total (H I + H_2) gas content, and consequently we restrict our analysis to the H I content alone. The presence of atomic hydrogen is not a sufficient condition for star formation processes to take place, however Kennicutt showed that the empirical correlation between SFR and gas content, when considering integrated quantities, is stronger for H I than for H_2 taken alone.

Figure 2 shows the dependence of Hα EW on the hybrid H I surface density, in our sample. The H I surface density has been computed dividing the total integrated H I mass by the area of the galaxy, derived from the optical major axis, as given in the UGC or accordingly determined.

Using hybrid H I surface density is in principle inappropriate for comparing unperturbed galaxies with cluster objects suffering from H I deficiency. In fact, Warmels (1986) and Cayatte et al. (1990) showed that the gas is removed preferentially from the outer disk in deficient objects, producing a relevant change in their H I disk diameter. Using the sample of 96 galaxies having well-resolved H I observations presented in Warmels (1986), we estimate the change in the isophotal H I diameter with respect to the optical diameter, as a function of the projected distance from the Virgo Cluster center. On the average, galaxies with projected distances of more than 2° from M87 (all non–H I–deficient objects) have H I diameters 1.5 times larger than the optical ones. Galaxies in the inner 2° region (preferentially H I–deficient objects) have comparable H I and optical disks, the average ratio of the two diameters being 0.98. Therefore, adopting the hybrid definition of H I surface density, we derive realistic values for cluster objects, while we overestimate by a factor of about 2 the real surface density in isolated galaxies. The effect is relatively small, and no correction has been applied to the data presented in Figure 2. The noncluster objects (*empty circles*), although with a considerable scatter, are found compatible with the nonlinear regime discussed by Kennicutt (1989), showing a gas surface density close to the threshold value discussed earlier. However, the agreement might be fortuitous since the threshold column density is a strong function of radius within any individual galaxy, and therefore can be determined with confidence only in spatially resolved objects, while our H I surface densities are averages

TABLE 3

AVAILABLE PHOTOMETRICAL MEASUREMENTS FOR 883 SPIRAL GALAXIES

	ALL		WITH H MAG	
BAND	Surveyed	Detected	Surveyed	Detected
H I	692	603	490	444
Radio continuum	653	210	429	170
FIR	856	507	528	369

© American Astronomical Society • Provided by the NASA Astrophysics Data System

1993ApJ...409..110S

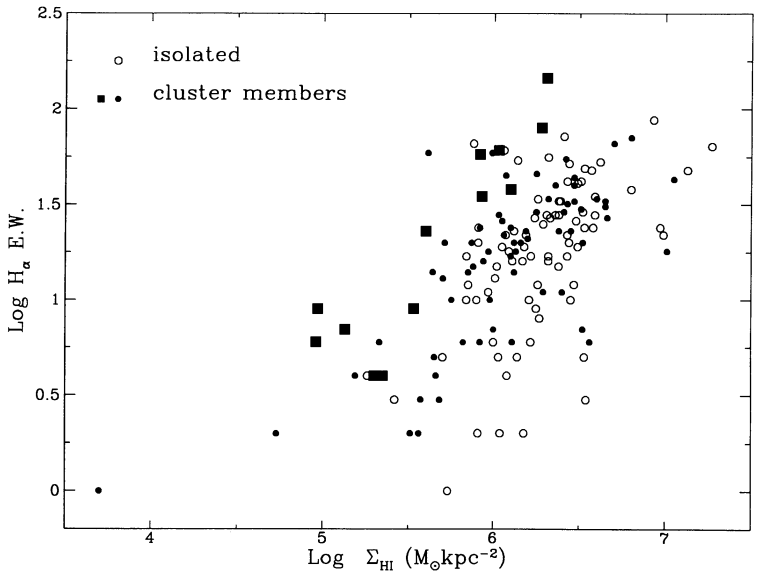

FIG. 2.—The relation between the Hα EW and the hybrid H I surface density for isolated (*open symbols*) and cluster galaxies (*filled symbols*). Filled squares are galaxies showing excess radio-continuum emission discussed in §§ 3.2 and 3.3. Many upper limits to the H I surface density of cluster galaxies are not shown for simplicity.

taken over an entire disk. Keeping this caution in mind, we notice that the relation in the cluster sample (*filled circles and squares*) is significantly different. There are many objects which overlap with the noncluster galaxies, but a significant number of objects with H I surface density as much as two orders of magnitude lower (the well-known H I–deficient cluster galaxies, see Giovanelli & Haynes 1985), have "normal" rates of star formation. For normal rates we mean similar to those observed in galaxies with normal H I content, thus having gas density from 10 to 100 times higher. We conclude that the cluster membership has the well-known observable influence on the H I gas content, but little or no consequence on the average SFR. In fact the distribution of Hα EW in the two samples are statistically indistinguishable (Fig. 3*a*). On the contrary the distribution of H I surface densities in cluster galaxies is significantly skewed toward lower densities relative to the nearly Gaussian distribution of noncluster objects (Fig. 3*b*). The probability that the two distributions are drawn from the same parent population is less than 10^{-10}, as given by a two-tailed Kolmogorov-Smirnov test. The test has been applied to the total H I sample of 360 cluster and 330 isolated galaxies. It should be remembered, however, that the above finding that cluster and isolated galaxies are indistinguishable in their star formation properties contains a possible bias. Here we are considering only galaxies exhibiting spiral morphology *at the present time* (inside and outside clusters). If many of the S0 galaxies presently seen in clusters were in the past spirals in which the SFR was quenched due to gas removal, they should be included in the cluster sample together with the galaxies still exhibiting a spiral morphology (and some residual SFR). Their inclusion would lower the mean of the Hα distribution in the cluster sample more than that of the noncluster sample.

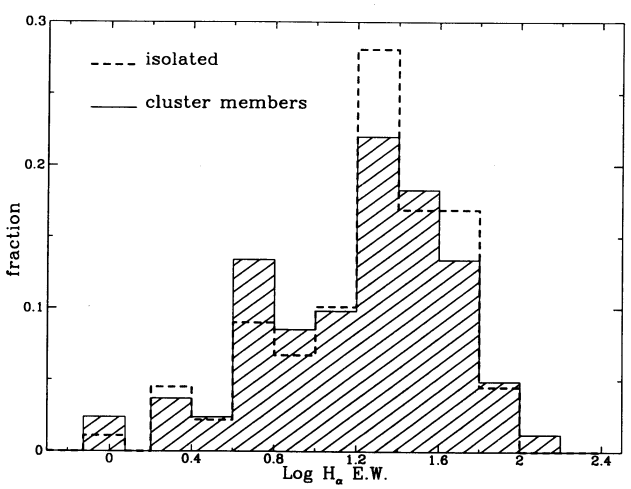

FIG. 3*a*

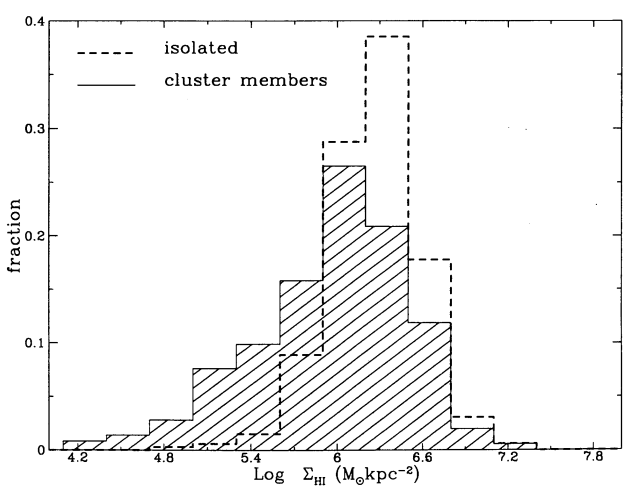

FIG. 3*b*

FIG. 3.—Frequency distribution of (*a*) the Hα EW, and (*b*) the H I surface density, in the isolated and in the cluster sample. The total number of objects has been normalized to one in both samples. Upper limits, which are frequent among cluster galaxies in (*b*), are treated as detections.

© American Astronomical Society • Provided by the NASA Astrophysics Data System

1993ApJ...409..110S

We interpret the presence of normal SFR in gas-deficient objects as a consequence of the different distribution of molecular and of H I gas in spiral disks. The denser and more centrally condensed molecular clouds, which give birth to stars, are not as easily stripped as the diffuse H I: it was in fact shown that H I–deficient objects in clusters have normal molecular gas content (Kenney 1990; Casoli et al. 1991). Therefore, even though in these galaxies a significant fraction of the H I has been removed, the star formation activity goes on until it is sustained by the molecular gas supply. This could be as long as some 10^9 yr (Larson & Tinsley 1978). The typical time scale for H I stripping is 1–4 × 10^8 yr (Lea & De Young 1976; Nulsen 1982). Gavazzi (1989), arguing that the H I asymmetry observed in three cluster galaxies is a transient phenomenon, soon washed out by galaxy differential rotation, was able to confirm the time scale for ablation in few times 10^8 yr.

We conclude that these galaxies must have resided in the hostile cluster environment for a time longer than the typical time scale for stripping but shorter than some 10^9 yr, i.e., that these galaxies are relatively recent cluster "intruders."

At the total consumption of molecular hydrogen, unless other forms of gas replenishment would compensate for the missing supply of H I, the star formation activity in these galaxies will eventually suffer a drastic decrease. Those objects that are cluster members since the time of cluster formation would populate the lower left part of Figure 2. However, due to incompleteness of the Hα survey and to the limited sensitivity of the present H I observations, they cannot be detected. Could S0 galaxies that we presently observe in clusters be the product of this final evolution, as proposed by Larson, Tinsley, & Caldwell (1980)? A systematic survey of the star formation properties and of the residual gas content of cluster galaxies in the various morphological classes is necessary to solve this question. The upgraded Arecibo telescope might provide us with the proper sensitivity for this purpose.

A possible alternative scenario to explain the presence of normal SFR in H I–deficient objects, that we do not explore in this paper, is the one where a strong localized star formation activity induced by the ram pressure sweeping of the gaseous disk compensate the diffuse decrease in the SFR originated by the removal of the gas.

3.2. H I *Content and Synchrotron Emission*

The origin of the nonthermal radio emission in spiral galaxies is not fully understood, but general agreement exists on the major role played by supernovae explosions of young massive stars in accelerating the relativistic electrons responsible for the radio emission (Klein 1982; Kennicutt 1983b; Gavazzi, Cocito, & Vettolani 1986; Burstein, Condon, & Yin 1987; Fitt, Cox, & Cox 1988; Gavazzi, Boselli, & Kennicutt 1991 [hereafter GBK91]). This hypothesis is supported by the observed correlation between the radio continuum emission and the star formation indicator Hα EW (Kennicutt 1983b; Gavazzi 1988, 1991; GBK91). Radio continuum emission is significantly environment dependent. Enhancements of the circumnuclear emission is observed in interacting pairs (Condon et al. 1982; Altschuler & Pantoja 1984) and the diffuse disk emission has been reported to be enhanced in cluster galaxies (Gavazzi & Jaffe 1986; Gavazzi 1988, 1991; GBK91).

As a consequence of the correlation between radio continuum emission and SFR, and of the dependence of this latter on the H I surface density discussed in the previous paragraph, it is not surprising that the radio continuum versus H I surface density relation follows a pattern similar to the one in Figure 2. In Figure 4 the ratio radio/*H* is plotted versus the hybrid H I surface density. Only objects detected in the radio continuum are plotted, upper limits being evenly distributed over the whole ranges of radio/*H* and of H I surface density covered by the detected objects, thus adding no useful information. The scatter present in the correlation is large, due to the nondirect physical link between the two plotted quantities. If the cluster and the noncluster samples are considered separately, it appears that the scatter is larger among cluster members (*filled circles*). In this sample nearly two-thirds of the objects are indistinguishable from noncluster galaxies (*open circles*), but there is a number of objects having a radio emission greater than any noncluster object at any given H I surface density.

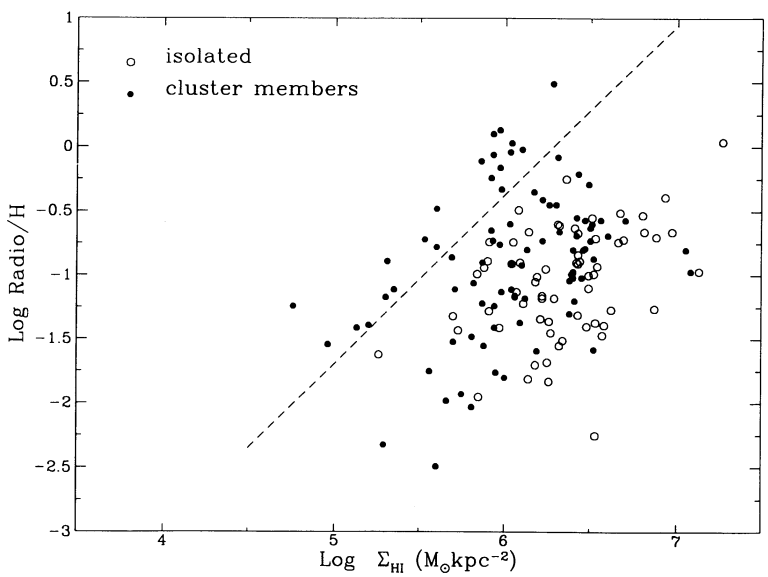

FIG. 4.—The relation between the radio/*H* ratio and the hybrid H I surface density for isolated (*open symbols*) and cluster galaxies (*filled symbols*). The meaning of the dotted line is discussed in the text. Many upper limits to the H I surface density of cluster galaxies are not shown for simplicity.

© American Astronomical Society • Provided by the NASA Astrophysics Data System

1993ApJ...409..110S

TABLE 4

CLUSTER GALAXIES WITH RADIO EXCESS

Name (1)	NGC (2)	Opt (3)	H I (4)	R.C. (5)	HISd (6)	rad/H (7)	Cluster (8)
522041.....	710	Yes	?	No	5.86	−0.11	A262
97087.....	...	Yes	Yes	Yes	6.03	−0.04	A1367
97073.....	...	Yes	Yes	Yes	6.28	0.49	A1367
97079.....	...	Yes	Yes	Yes	6.31	−0.08	A1367
97120.....	3860	No	?	No	5.30	−1.17	A1367
160260.....	4911	Yes	Yes	Yes	5.53	−0.72	Coma
160064.....	...	No	?	Yes	5.98	−0.33	Coma
160095.....	4921	Yes	Yes	Yes	5.13	−1.41	Coma
160015.....	...	No	?	Yes	<5.60	−0.78	Coma
160086.....	...	Yes	?	No	5.92	−0.24	Coma
160252.....	4040	Yes	No	No	5.93	0.10	Coma
160098.....	...	No	No	Yes	5.97	−0.16	Coma
160108.....	...	Yes	?	No	<6.04	0.03	Coma
160055.....	4848	Yes	Yes	Yes	5.60	−0.48	Coma
99075.....	4498	No	Yes	?	5.97	0.13	Virgo
70197.....	4579	No	Yes	No	5.35	−1.11	Virgo
70192.....	4569	Yes	Yes	No	4.96	−1.54	Virgo
70068.....	4388	Yes	Yes	Yes	5.31	−0.89	Virgo
70097.....	4438	Yes	Yes	Yes	4.76	−1.24	Virgo (Double sys)
160213.....	4858	Yes	?	No	<5.93	−0.06	Coma (Double sys)
160096.....	4922	Yes	?	No	6.10	−0.02	Coma (Double sys)

To understand the origin of this larger scatter, we draw in Figure 4 an arbitrary line such that all noncluster objects lie below it. This line cuts the cluster sample in two parts: below the line there are cluster objects indistinguishable from isolated galaxies (comparison cluster sample), above the line there are 21 cluster objects which show extreme radio properties at any given H I surface density. These cluster galaxies include many radio faint objects, nevertheless showing a radio/H ratio 3–5 times higher than expected from the H I surface density of relatively isolated galaxies taken as a reference. The 21 cluster galaxies showing excess radio emission are listed in Table 4, while Table 5 list the 11 galaxies in the comparison cluster sample showing the lowest values of radio/H for a given H I surface density. In these tables we list possible evidences of overall disturbances in the galaxy morphology: a "yes" in column (3) indicates the presence of optical asymmetries (such as evidences of disrupted disks, presence of abnormal arms); asymmetries in the H I distribution (offsets from the galaxy centers derived from H I maps or strong asymmetries derived from H I profiles for spatially unresolved objects) are indicated by a "yes" in column (4); asymmetries or offsets in the radio continuum morphology are given with a "yes" in column (5).

TABLE 5

CLUSTER COMPARISON SAMPLE

Name (1)	NGC (2)	Opt (3)	H I (4)	R.C. (5)	HISd (6)	rad/H (7)	Cluster (8)
522086.....	753	No	No	Yes	6.41	−1.20	A262
97091.....	3840	No	No	No	6.38	−1.30	A1367
160148.....	...	No	No	No	6.00	−1.80	Coma
43071.....	4808	No	No	No	7.05	−0.80	Virgo
129027.....	4725	No	Yes	No	5.81	−2.03	Virgo
70194.....	4571	No	No	No	5.75	−1.93	Virgo
129010.....	4565	No	No	No	5.95	−1.76	Virgo
99044.....	4383	No	No	No	7.08	−0.97	Virgo
100004.....	4651	No	No	No	6.52	−1.58	Virgo
157041.....	3912	No	No	No	6.19	−1.59	Virgo
69112.....	4216	No	No	No	5.60	−2.49	Virgo

We consider significant an offset of more than 10″ between the optical and radio coordinates (corresponding to $\approx 3.6\ h^{-1}$ kpc at the typical distance of these galaxies, except for Virgo members, where it corresponds to $\approx 0.6\ h^{-1}$ kpc). Question marks indicate undecidable cases, where some relevant information is missing in the published data. The tables also report the quantities plotted in Figure 4 (H I surface density and radio/H, in cols. [6] and [7]). Three galaxies showing excess radio emission are double systems or have companions of comparable magnitude. Tidal interaction is probably the best explanation for their excess radio emission. Of the remaining 18, 12 show optical asymmetries, 10 asymmetries in the H I distribution, three clear radio continuum trails, and other six radio-optical positional offsets (notice, however, that the resolution of the available radio continuum observations is very inhomogeneous: for example, Coma Cluster galaxies have never been observed with the proper resolution (5″–10″) and sensitivity to allow to detect asymmetries or significant optical-radio offsets).

Among the 11 galaxies in Table 5 only one (129027 = NGC 4725) shows H I asymmetry, and one (522086 = NGC 753) has a radio/optical offset; the remaining have normal morphologies. We conclude that there is strong evidence that galaxies showing enhanced radio activity are found among those cluster members with significant disturbances. Conversely these objects are virtually absent among the comparison cluster sample and among the isolated galaxies.

Examples of disturbed galaxies in Table 4 are: 97073-79-87 at the northwest periphery of A1367. Radio continuum trails were detected by Gavazzi & Jaffe (1987) and H I asymmetry was found by Gavazzi (1989) and by Dickey & Gavazzi (1991). Object 160055 (NGC 4848), 160260 (NGC 4911), and 160095 (NGC 4921) in the Coma Cluster have H I asymmetry reported by Gavazzi (1989) and by Sullivan (1989). Notice that five of the seven blue galaxies in the Coma Cluster reported by Bothun & Dressler (1986) as possible examples of galaxies whose star formation was enhanced by ram-pressure, belong to this list. Object 99075 (NGC 4498), 70068 (NGC 4388), 70192

© American Astronomical Society • Provided by the NASA Astrophysics Data System

1993ApJ...409..110S

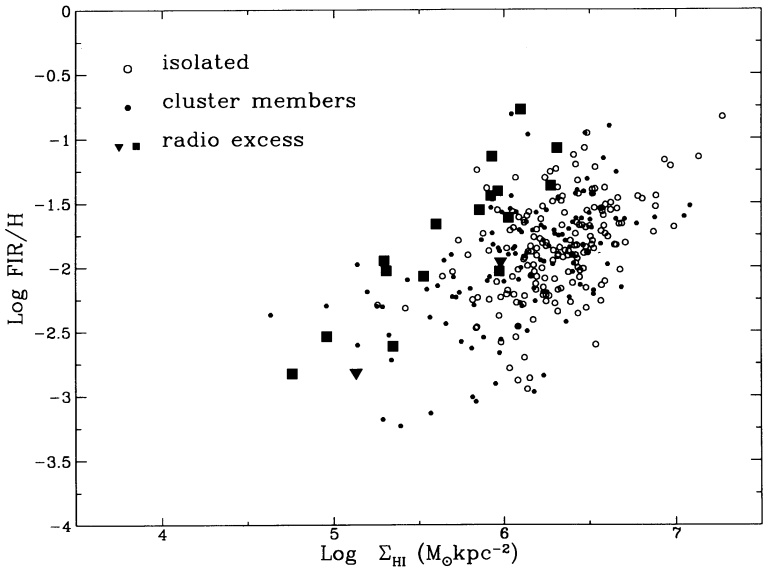

FIG. 5.—Relation between the FIR/*H* ratio and the hybrid H I surface density for isolated (*open symbols*) and cluster galaxies (*filled symbols*). Filled squares and triangles are galaxies showing excess radio-continuum emission, for which the ratio FIR/*H*, or an upper limit to the ratio, respectively, is available.

(NGC 4569),[3] and 70197 (NGC 4579) in the Virgo Cluster were found asymmetric in the H I maps by Cayatte et al. (1990) and/or by Warmels (1986). Eight of the 21 galaxies in Table 3 were discussed in Dickey & Gavazzi (1991) as possible examples of ram pressure-swept galaxies. This evidence reinforces the argument of Bothun & Dressler (1986), Gavazzi (1989), and Dickey & Gavazzi (1991) that ram pressure occurring in clusters of galaxies, along with producing stripping of the gaseous component associated with their disks, might as well be responsible for morphological disturbances and radio continuum enhancements.

3.3. *Synchrotron Emission and Star Formation*

Given the correlation between radio continuum emission and star formation activity discussed in § 3.2, it seems reasonable to assume, in first approximation, that enhanced SFR could produce the observed enhanced radio continuum activity among the galaxies listed in Table 4. Measurements of the Hα EW are available for only 13 of the 21 galaxies (indicated with filled squares in Fig. 2). It is apparent that these galaxies have, on average, a strong SFR for their gas content. To decide whether this high SFR could entirely explain the increase in the radio continuum activity, we examine the correlation between FIR, taken temporarily as another star formation indicator, and the H I surface density. This is shown in Figure 5, where the ratio FIR/*H* is plotted against H I surface density. A general correlation between the plotted quantities is not surprising (see Spitzak & Schneider 1992). Empty circles represent isolated galaxies and filled symbols represent cluster objects. Filled squares represent those galaxies among the 21 of Table 4 for which the ratio FIR/*H* is available (the triangles mark two upper limits within these 21 objects). At any given H I surface density these objects have high FIR/*H* ratios, but not as extreme as their radio/*H*, indicating that FIR is not as enhanced as the radio continuum, among the disturbed objects.

[3] The asymmetry is visible only in the global line profile, and is not evident in the Cayatte et al. map (see their Fig. 14*f*).

In spite of the tight correlation found between radio continuum and FIR integrated luminosities (Dickey & Salpeter 1984; Helou, Soifer, & Rowan-Robinson 1985; Gavazzi et al. 1986) and surface brightness distributions (Bicay & Helou 1990), we conclude that, unless the characteristic time scales for radio continuum and FIR enhancements are considerably different, an increase in star formation activity cannot entirely explain the radio continuum enhancements in cluster spirals. Another mechanism is required.

To better quantify this point, we examine in Figure 6*a* the correlation between the ratio radio/*H* and the Hα EW. The least-squares fit between the two quantities is

$$\log (\text{radio}/H) = -2.14 + 0.91 \log \text{H}\alpha(\text{EW})$$

(see GBK91 for details on the derivation). Figure 6*b* shows that all the "radio-excess" galaxies listed in Table 4 have positive residuals with respect to the correlation, having a ratio radio/*H* systematically higher than expected from their Hα EW. A similar analysis using FIR/*H* and Hα EW is shown in Figure 7*a*. The least-squares fit between the two quantities is

$$\log (\text{FIR}/H) = 0.35 + 0.72 \log \text{H}\alpha(\text{EW}) .$$

Figure 7*b* shows that, on average, galaxies with radio excess have no net residual with respect to the derived correlation, instead that their ratio FIR/*H* is consistent with the one expected from their Hα EW.

4. SUMMARY AND CONCLUSIONS

The main results of this work can be summarized as follows.

1. The average SFR in cluster galaxies is normal, in spite of the fact that their H I hybrid surface density is as much as two orders of magnitude lower than that of isolated galaxies (Figs. 2 and 3).

2. A significant fraction of cluster galaxies shows a radio continuum excess as compared with isolated galaxies of similar gas content (Fig. 4). Morphological disturbances seem to characterize these objects.

© American Astronomical Society • Provided by the NASA Astrophysics Data System

1993ApJ...409..110S

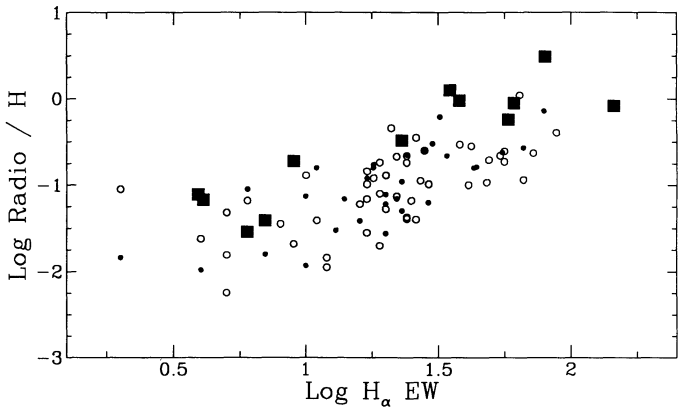

FIG. 6a

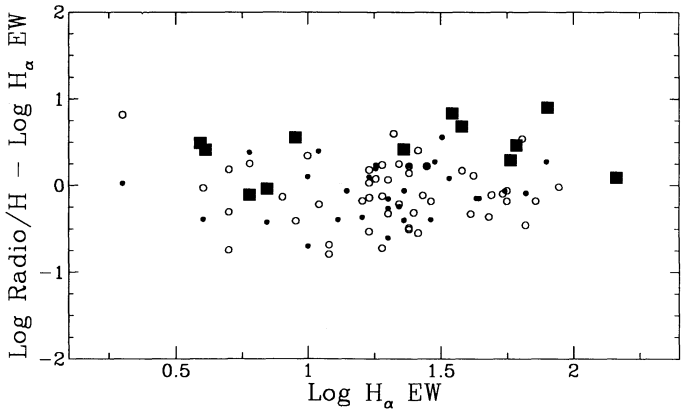

FIG. 6b

FIG. 6.—Correlation between the radio/H ratio and the Hα EW (*a*) and the residuals with respect to the linear regression discussed in the text (*b*). Same symbols as in the previous figure.

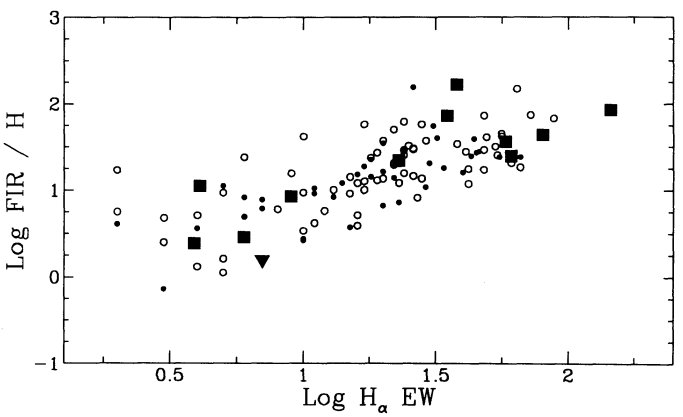

FIG. 7a

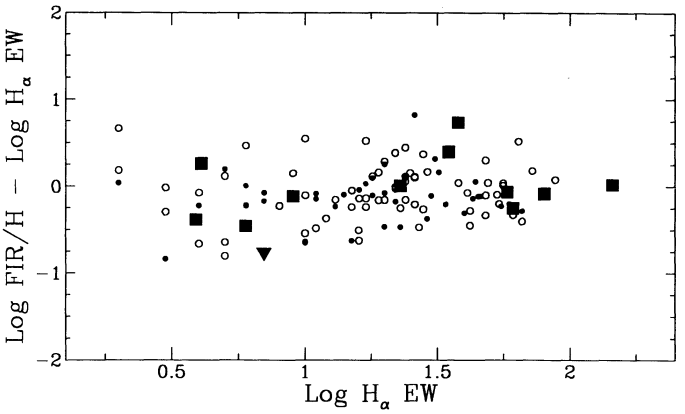

FIG. 7b

FIG. 7.—Correlation between the FIR/H ratio and the Hα EW (*a*) and the residuals with respect to the linear regression discussed in the text (*b*). Same symbols as in the previous figures.

3. Cluster galaxies with radio excess have rather high SFR, as indicated by their FIR emission at any given H I surface density (Fig. 5).

4. However a radio enhancement is observed in disturbed cluster spirals spanning a large range of Hα EW (Fig. 6) and it is much more pronounced than the corresponding FIR enhancement (Fig. 7).

We conclude that enhanced SFR in disturbed cluster systems does not entirely account for the observed radio continuum excess. Another mechanism is required to produce an extra enhancement of the synchrotron emissivity. We argue that magnetic field compression induced by the dynamical interaction between the fast moving galaxies and the hot, dense intergalactic medium (IGM) might explain these radio continuum enhancements that have no corresponding FIR enhancements. In fact, the synchrotron emissivity ϵ due to cosmic ray electrons depends on the density of relativistic electrons n_e, which is in turn proportional to the galaxy SFR (GBK91), and on the intensity of the magnetic field H as $\epsilon = n_e H^\alpha$ with $\alpha \approx 2$. The observed average 3–5 times enhancement of ϵ in cluster spirals could be explained if magnetic field amplification by a factor of 2 would be induced in those cluster galaxies suffering from ram pressure.

Well-documented disturbances to the magnetic field structure induced by the interaction with the IGM in clusters of galaxies occur in the "head-tail" radio sources, often found associated with bright elliptical galaxies. Less spectacular, though observable magnetic field distortions are detected in the irregular galaxies 97073 and 97079 in A1367 (Gavazzi & Jaffe 1987). Higher resolution and sensitivity observations of the objects listed in Table 4 are necessary to detect similar phenomena.

M. S. acknowledges a grant from the University of Milano which made possible his stay at the Arecibo Observatory for 1 month. We are indebted to the Director of the Arecibo Observatory for his hospitality during our stay at the Observatory and to the telescope operators for their collaboration. We wish to thank R. Giovanelli for providing us with some observations of A262 galaxies prior to publication, for assistance in the observations and for useful comments on the manuscript; W. Freudling for assistance in the data reduction; J. Dickey and R. Kennicutt for helpful conversations and comments on an early version of this paper. A special thanks is due to A. Boselli for his precious contributes to the discussion.

© American Astronomical Society • Provided by the NASA Astrophysics Data System

1993ApJ...409..110S

REFERENCES

Altschuler, D., & Pantoja, C. 1984, AJ, 89, 1531
Basso, L., Palumbo, G., Primavera, R., Vettolani, G., & Vigotti, M. 1990, A&AS, 83, 569
Bicay, M., & Helou, G. 1990, ApJ, 362, 59
Bothun, G., Aaronson, M., Schommer, R., Huchra, J., Mould, J., & Sullivan, W. 1985, ApJS, 70, 271
Bothun, G., & Dressler, A. 1986, ApJ, 301, 57
Burstein, D., Condon, J., & Yin, Q. 1987, ApJ, 315, L99
Casoli, F., Boisse, P., Combes, F., & Dupraz, C. 1991, A&A, 249, 359
Cayatte, V., Van Gorkom, J., Balkowski, C., & Kotanyi, C. 1990, AJ, 100, 604
Condon, J., Condon, M., Gisler, G., & Pushell, J. 1982, ApJ, 252, 102
Cox, P., Krugel, E., & Mezger, P. 1986, A&A, 155, 407
de Vaucouleurs, G., de Vaucouleurs, A., Corwin, H., Buta, R., Paturel, G., & Fouque, P. 1991, Third Reference Catalogue of Bright Galaxies (New York: Springer) (RC3)
Dickey, J., & Gavazzi, G. 1991, ApJ, 373, 347
Dickey, J., & Salpeter, E. 1984, ApJ, 248, 461
Fitt, A., Cox, P., & Cox, M. 1988, MNRAS, 233, 407
Gavazzi, G. 1987, ApJ, 320, 96 (Paper I)
———. 1988, in The Minnesota Lectures on Clusters of Galaxies and Large-Scale Structure, ed. J. Dickey (ASP Conf. Ser., 5), 115
———. 1989, ApJ, 346, 59 (Paper II)
———. 1991, in IAU Symp. 146, Dynamics of Galaxies and their Molecular Cloud Distribution, ed. F. Combes & F. Casoli (Dordrecht: Kluwer), 403
Gavazzi, G., Boselli, A., & Kennicutt, R. 1991, AJ, 101, 1207 (GBK91)
Gavazzi, G., Cocito, A., & Vettolani, G. 1986, ApJ, 305, L15
Gavazzi, G., & Jaffe, W. 1986, ApJ, 310, 53
———. 1987, A&A, 186, L1
Gavazzi, G., Scodeggio, M., Boselli, A., & Trinchieri, G. 1991b, ApJ, 382, 19
———. 1992, A&A, 258, 265
Giovanelli, R., & Haynes, M. 1985, ApJ, 292, 404
Giovanelli, R., & Haynes, M. 1989, AJ, 97, 633
Guiderdoni, B. 1987, A&A, 172, 27
Haynes, M., Giovanelli, R., & Chincarini, G. 1984, ARA&A, 22, 445
Helou, G., Soifer, B., & Rowan-Robinson, M. 1985, ApJ, 298, L7
Kenney, J. 1990, in The Interstellar Medium in Galaxies, ed. A. Thronson & J. Shull (Dordrecht: Kluwer), 151
Kennicutt, R. 1983a, A&A, 120, 219
———. 1983b, ApJ, 272, 54
———. 1989, ApJ, 344, 685
———. 1990, in The Interstellar Medium in Galaxies, ed. A. Thronson & J. Shull (Dordrecht: Kluwer), 405
Klein, U. 1982, A&A, 15, 42
Larson, R., & Tinsley, B. 1978, ApJ, 219, 46
Larson, R., Tinsley, B., & Caldwell, N. 1980, ApJ, 237, 692
Lea, S., & De Young, D. 1976, ApJ, 210, 647
Nilson, P. 1973, Uppsala General Catalogue of Galaxies (Uppsala: Obser. Annu., Vol. 6) (UGC)
Nulsen, P. 1982, MNRAS, 198, 1007
Santagata, N., Basso, L., Gottardi, M., Palumbo, G., Vettolani, G., & Vigotti, M. 1987, A&AS, 70, 191
Schmidt, M. 1959, ApJ, 129, 243
Spitzak, J., & Schneider, S. 1992, ApJ, 393, 126
Sullivan, W. 1989, in The World of Galaxies, ed. H. Corwin & A. Bottinelli (New York: Springer), 404
Sullivan, W., Bothun, G., Bates, B., & Schommer, R. 1981, AJ, 86, 919
Tully, B., & Fisher, R. 1977, A&A, 54, 661
Warmels, R. 1986, Ph.D. thesis, Groningen Univ.
Williams, B. 1986, ApJ, 311, 25
Young, J., & Scoville, N. 1991, ARA&A, 29, 581
Zwicky, J., et al. 1961–1968, Catalogue of Galaxies and Clusters of Galaxies (Pasadena: California Institute of Technology) (CGCG)

© American Astronomical Society • Provided by the NASA Astrophysics Data System